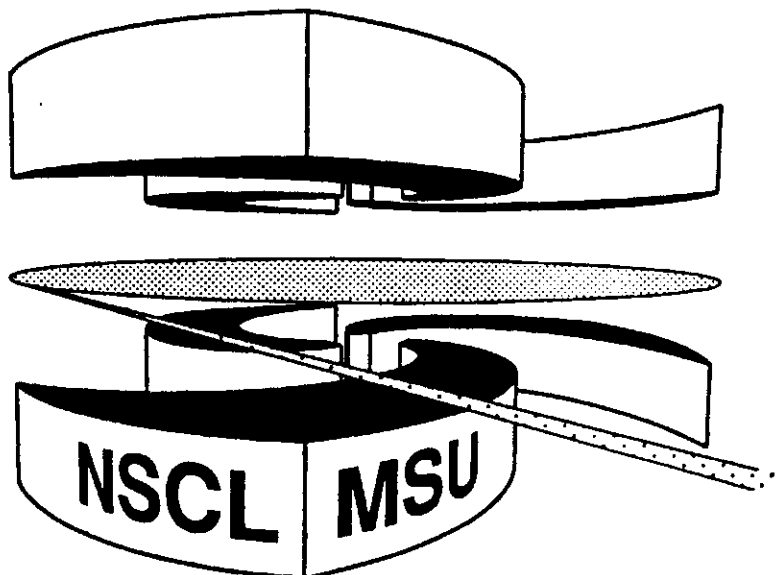


**MICHIGAN STATE  
UNIVERSITY**

**National Superconducting Cyclotron Laboratory**

**GROUND-STATE MAGNETIC MOMENT OF THE  $T = 1$   
NUCLEUS  $^{32}\text{Cl}$  USING ON-LINE  $\beta$ -NMR SPECTROSCOPY**

**W.F. ROGERS, G. GEORGIEV, G. NEYENS, D. BORREMANS,  
N. COULIER, R. COUSSEMENT, A. DAVIES, J. MITCHELL,  
S. TEUGHEL, B.A. BROWN, P.F. MANTICA**



SCAN-0009231



CERN LIBRARIES, GENEVA

MSUCL-1170

JULY 2000

# Ground-State Magnetic Moment of the $T = 1$ Nucleus $^{32}\text{Cl}$ Using On-Line $\beta$ -NMR Spectroscopy

W.F. Rogers<sup>(1)</sup>, G. Georgiev<sup>(2)</sup>, G. Neyens<sup>(2)</sup>, D. Borremans<sup>(2)</sup>, N. Coulier<sup>(2)</sup>,  
R. Coussement<sup>(2)</sup>, A. Davies<sup>(1)</sup>, J. Mitchell<sup>(1)</sup>, S. Teughels<sup>(2)</sup>, B.A. Brown<sup>(3)</sup>, P.F. Mantica<sup>(4)</sup>

<sup>(1)</sup> *Department of Physics, Westmont College, Santa Barbara, California 93108 USA*

<sup>(2)</sup> *University of Leuven, Instituut voor Kern- en Stralingsfysika, Celestijnenlaan 200 D, B-3001  
Leuven, Belgium*

<sup>(3)</sup> *National Superconducting Cyclotron Laboratory and Department of Physics and Astronomy,  
Michigan State University, East Lansing, Michigan 48824, USA*

<sup>(4)</sup> *Department of Chemistry and National Superconducting Cyclotron Laboratory, Michigan State  
University, East Lansing, Michigan 48824, USA*

(July 11, 2000)

## Abstract

The magnetic dipole moment of the  $1^+$  ground state of the  $T = 1$  nucleus  $^{32}_{17}\text{Cl}_{15}$  has been measured to be  $\mu = 1.114(6) \mu_N$  using conventional  $\beta$ -NMR spectroscopy. Polarized  $^{32}\text{Cl}$  nuclei were produced by fragmentation of a 100 MeV/nucleon  $^{36}\text{Ar}$  beam in a 642 mg/cm<sup>2</sup>  $^{93}\text{Nb}$  target, where the beam was incident on the target at an angle 2.5° to the normal beam axis. The desired  $^{32}\text{Cl}$  fragments were filtered from other fragmentation products using the A1200 fragment separator and implanted in a NaCl single crystal, maintained at room temperature, at the center of a  $\beta$ -NMR apparatus. The Larmor frequency was determined by measuring the  $\beta$ -decay asymmetry as a function of the applied radiofrequency field. Isoscalar and isovector moments for the  $A = 32$ ,  $T = 1$  isospin multiplet are extracted and compared with large-basis shell model calculations.

## I. INTRODUCTION

The measurement of nuclear magnetic dipole moments has played an important role in the investigation of nuclear structure. Nuclei around  $N = Z$ , especially as they become further removed from stability with increasing mass, have been of great theoretical interest, and a testing ground for charge symmetry and charge independence of nuclear forces. Nuclear magnetic dipole moments, as well as  $\gamma$ -decay transition rates and Gamow-Teller (GT)  $\beta$ -decay strengths, provide a sensitive probe into the single-particle nature of nuclei and the structure of nuclear wave functions, particularly in light nuclei in the  $sd$ - and  $f_{7/2}$ -shells. Attempts to account for discrepancies between measured magnetic moments and the single-particle model predictions are often approached in terms of configuration mixing, including core polarization and mesonic exchange.

Magnetic dipole moment measurements within isospin multiplets ( $T_z = (Z - N)/2$ ) are of particular interest, owing to the first-order similarity of nuclear structure between members. The roles of protons and neutrons are simply interchanged in two conjugate members of the multiplet, for which the Coulomb force can be neglected in first approximation. The isoscalar and isovector contributions, readily extracted by taking the sum and differences between members of opposite isospin  $\tau_z$ -projection, provide valuable information on nuclear structure. Although the ground state magnetic dipole moments for  $T = 1/2$  mirror partners have been determined for all bound nuclei up to  $A = 41$ , only limited magnetic moment information is available for members of  $T = 1$  multiplets. The ground state magnetic moments of both the  $T_z = +1$  and  $T_z = -1$  members of the  $T = 1$  multiplet have been experimentally deduced only for  $A = 8, 12, 20$ , and  $36$ . Such measurements are made difficult by the short decay half-lives and low production rates for the  $\beta$ -unstable  $T_z = +1$  nuclides which constitute  $T = 1$  multiplets.

Particularly useful in the study of magnetic moments of  $\beta$ -unstable nuclei has been the application of  $\beta$ -detected nuclear magnetic resonance ( $\beta$ -NMR). The use of  $\beta$ -NMR spectroscopy requires polarization of the nuclear spin ensemble. Several techniques have been

developed to produce spin-oriented (aligned and/or polarized) short-lived nuclei [1–4,6–8]. Generally, the most straightforward way to obtain spin-oriented nuclei is from the nuclear production reaction itself. It has been shown that the reaction products from fusion-evaporation reactions [1,2], as well as from projectile fragmentation reactions [4,5], are spin-oriented.

In conventional  $\beta$ -NMR experiments, the polarized nuclei are implanted in a crystal host (typically cubic) immersed in an external magnetic holding field, and nuclear polarization is monitored via the asymmetric angular distribution of the parity-violating  $\beta$ -decay. Since no electric field gradient is present at the cubic implantation sites, a regular Zeeman splitting between magnetic substates occurs as a function of  $B_0$  and nuclei precess at the single Larmor frequency  $\nu_L = g\mu_N B_0/h$ , where  $g$  is the nuclear  $g$  factor,  $\mu_N$  is the nuclear magneton,  $B_0$  is the magnetic holding field, and  $h$  is Planck's constant. Nuclear level populations can be modified by application of an orthogonal radiofrequency (RF) magnetic field, whose frequency matches the Larmor precession frequency at the particular  $B_0$ . The magnetic dipole moment  $\mu$  can be deduced from the nuclear  $g$  factor if the nuclear spin  $I$  is known. The  $\beta$ -NMR method is well-suited for studying short-lived nuclei since the  $\beta$  decay must occur before relaxation of the nuclear spin-orientation, which is typically on the order of a few seconds.

We report here on the measurement magnetic dipole moment of the  $T_{1/2} = 298$  ms ground state of  ${}^{32}_{17}\text{Cl}_{15}$  using  $\beta$ -NMR spectroscopy coupled with the production of spin-polarized beams from intermediate-energy projectile fragmentation. The nucleus  ${}^{32}\text{Cl}$  is the  $T_z = +1$  member of the  $A = 32$ ,  $T = 1$  multiplet, which also includes  ${}^{32}_{15}\text{P}_{17}$  ( $T_z = -1$ ) and an excited state of  ${}^{32}_{16}\text{S}_{16}$  ( $T_z = 0$ ). The experimental determination of the  ${}^{32}\text{Cl}$  ground state magnetic moment allows extraction of the isoscalar and isovector components of the dipole operator for this  $T = 1$  multiplet in the  $sd$ -shell.

## II. EXPERIMENTAL TECHNIQUE AND RESULTS

A radioactive beam of  $^{32}\text{Cl}$  at 36 MeV/nucleon was obtained using the A1200 fragment separator at the National Superconducting Cyclotron Laboratory (NSCL) at Michigan State University. A primary beam of  $^{36}\text{Ar}$  was accelerated to 100 MeV/nucleon using the K1200 cyclotron and fragmented in a 642-mg/cm<sup>2</sup> thick  $^{93}\text{Nb}$  target located at the object position of the A1200 separator. Two dipole magnets upstream from the  $^{93}\text{Nb}$  target were used to steer the primary beam 2.5° with respect to the normal beam axis [9]. A 425 mg/cm<sup>2</sup> Al wedge-shaped degrader with a slope angle of 3.5 mrad was placed at the second dispersive image of the A1200 to separate the fragment isotopes with given mass-to-charge ratio based on A and Z. The angular acceptance of the A1200 fragment separator is  $\sim 1^\circ$ , while the momentum acceptance was set to 1% using slits placed at the first dispersive image of the device.

Under the best conditions two different isotopes,  $^{32}\text{Cl}$  ( $T_{1/2} = 0.298$  s,  $Q_{EC} = 12.7$  MeV,  $J^\pi = 1^+$ ) and  $^{31}\text{S}$  ( $T_{1/2} = 2.572$  s,  $Q_{EC} = 5.4$  MeV,  $J^\pi = 1/2^+$ ), were identified in the secondary beam using the fragment energy loss and time-of-flight information. The ratio of the production rates of  $^{31}\text{S}:$  $^{32}\text{Cl}$  was nearly 2:1. The energy of this secondary beam was degraded to  $\approx 10$  MeV/nucleon using Al foils. The secondary beam was then collimated and implanted into a crystal host at the center of a  $\beta$ -NMR apparatus.

A schematic drawing of the NSCL  $\beta$ -NMR system [9] is shown in Fig. 1. An electromagnet with pole gap of 10.2 cm provided a holding field in the vertical direction. Two  $\beta$ -telescopes, each consisting of two 4.4 cm  $\times$  4.4 cm  $\times$  0.3 cm thick  $\Delta E$  and a 5.1 cm  $\times$  5.1 cm  $\times$  2.5 cm thick  $E$  plastic scintillators, were placed between the magnet poles at 0° and 180° with respect to the holding field. Acrylic light guides were used to direct the light from the scintillators to photomultiplier tubes positioned outside the magnetic field. A 2-mm thick NaCl single crystal, 2.5 cm in diameter was used as an implantation host. Two RF coils, each of 30-turn loops with radius 1.2 cm and separation 1.2 cm were arranged in a Helmholtz-like geometry about the NaCl crystal. The coil inductance was measured to be

51  $\mu H$  and the coils were arranged such that the resulting RF field was mutually perpendicular to the applied holding magnetic field and the direction of the secondary beam.

Measurements of the  $\beta$ -asymmetry as a function of the applied RF field were conducted using continuous implantation of the  $^{32}\text{Cl}$  nuclei [9]. The angular distribution of  $\beta$  particles is given as

$$W_{\beta}(\theta) = 1 + (v/c)AP\cos(\theta), \quad (1)$$

where  $\theta$  is the angle between the emitted positron relative to the spin axis of the nucleus,  $P$  is the polarization of the implanted ensemble,  $v/c$  is positron velocity divided by the speed of light, and  $A$  denotes the asymmetry parameter for the decay.

The RF was switched on and off in intervals 59.5 s and 60.5 s, respectively. The data acquisition (DAQ) cycles also consisted of two intervals, RF-on (60 s) and RF-off (60 s). Note that the RF-on application period was 0.5 sec shorter than the RF-on DAQ cycle. This allowed for the  $^{32}\text{Cl}$  ( $T_{1/2} = 0.298$  s) implanted during the cycle to decay away during the last 0.5 s of the RF-on DAQ cycle before the RF-off DAQ cycle began. Strength of the RF was 0.3(1) mT. The ratio of the counting rates in the  $0^{\circ}$  (up) and  $180^{\circ}$  (down)  $\beta$ -telescopes both for RF-on and RF-off conditions was calculated to reduce instrumental asymmetries. This ratio yields 1 for all points removed from resonance. Only in the vicinity of the resonance, where the change in  $\beta$ -asymmetry occurs, will this ratio deviate from 1.

Triple coincidences between  $\beta$ -telescopes were used to discriminate against detection of  $\gamma$ -rays. To avoid the influence of the  $^{31}\text{S}$  contaminant on the measured  $\beta$  asymmetry, an off-line energy discrimination was performed on the spectra collected in the thick  $\beta$  detectors. Since  $Q_{EC}(^{31}\text{S}) < Q_{EC}(^{32}\text{Cl})$ , only the higher energy part of the  $\beta$  spectra was used for the analysis. Use of this energy threshold also allowed discrimination of the mixed Fermi/GT transition  $^{32}\text{Cl}(1^+) \rightarrow ^{32}\text{S}(1^+)$  which is 20.5% [10] of the total intensity and has an unknown Fermi/GT mixing ratio. For this reduced portion of the  $\beta$ -decay spectrum the asymmetry factor was calculated to be  $A_1 = 0.31$  [11].

The experiment was conducted in two stages. During the first stage a search for the

resonance position was performed using a frequency modulation (FM) of  $\pm 25$  kHz ( $\Delta\nu/\nu \approx 3\%$ ). The holding field  $B_0$  was set to  $100.22(2)$  mT.

A scan of frequency over the range  $675 \pm 25$  kHz to  $975 \pm 25$  kHz corresponding to a total  $g$  factor range 0.85 to 1.31 produced the results depicted by open circles in Fig. 2(a). A deviation of greater than  $5\sigma$  in the asymmetry signal indicates the resonance position. The two filled circles in Fig. 2(a) were taken during the second stage of the experiment, which confirmed the first result.

To achieve better precision for the magnetic moment, a smaller FM value was employed in the second stage of the measurement. The holding field  $B_0$  was set to  $100.1(1)$  mT and the total frequency window  $835 \pm 10$  kHz to  $895 \pm 10$  kHz was scanned ( $\Delta\nu/\nu \approx 1\%$ ) corresponding to a  $g$  factor range 1.081 to 1.186, the results of which are depicted in Fig. 2(b). Two of the points in Fig. 2(b) show a clear change in the  $\beta$ -decay asymmetry and thus define the resonance position. Each of these two points overlaps somewhat with neighboring points which show no resonance change in  $\beta$ -decay asymmetry. Therefore, only the 10 kHz-wide frequency window shared by these two points alone defines the resonance location. The center of this window, 850 kHz, was used to deduce the  $^{32}\text{Cl}$  magnetic moment, yielding  $\mu = 1.114 \pm 0.006_{(\text{stat.})} \pm 0.001_{(\text{syst.})} \mu_N$ . The statistical error includes only the uncertainty from the frequency window of the FM, while the systematic error is mainly attributed to the uncertainty of the holding magnetic field.

### III. DISCUSSION

The nuclear magnetic dipole ( $M1$ ) operator is represented as the sum of two terms [12],

$$\mu = gJ\mu_N = \sum_i \langle JM | (g_l^{(i)} l_z^{(i)} + g_s^{(i)} s_z^{(i)}) | JM \rangle_{M=J} \mu_N \quad (2)$$

where  $\mu_N = e\hbar/2m_p$  is the nuclear magneton, and  $l^{(i)}$  and  $s^{(i)}$  are the orbital and spin angular momentum operators for the  $i^{\text{th}}$  nucleon. The total magnetic moment operator is summed over all  $A$  nucleons in the nucleus, and  $g_l^{(i)}$  and  $g_s^{(i)}$  are the orbital and spin gyromagnetic

ratios of the  $i^{\text{th}}$  nucleon. The free-nucleon values for the  $g$  factors are  $g_l^p = 1$ ,  $g_l^n = 0$ ,  $g_s^p = 5.5855$  and  $g_s^n = -3.826$ .

When the moments of the mirror pairs of nuclei are both known it is useful to compare the results for the isoscalar and isovector moments, which are linear combinations of the isospin multiplet moments:

$$\mu^s = \frac{1}{2} [\mu(T_z = +T) + \mu(T_z = -T)] \quad (3)$$

$$\mu^v = \frac{1}{2} [\mu(T_z = +T) - \mu(T_z = -T)]. \quad (4)$$

If one assumes good isospin and ignores the isoscalar exchange currents one can relate the isoscalar moment to the isoscalar spin expectation value [13,14]:

$$\mu^s = \frac{J}{2} + 0.38\langle s \rangle \quad (5)$$

where

$$\langle s \rangle = \sum_i \langle JM | s_z^{(i)} | JM \rangle_{M=J} \quad (6)$$

and where the factor 0.38 is the free-nucleon value for  $(g_s^n + g_s^p - g_l^p)/2$

For odd- $A$  nuclei, and in the extreme single-particle model, one can calculate the single-particle magnetic moment from (1) using the Landé theorem:

$$\mu_{sp} = \langle jm | [g_l j_z + (g_s - g_l) s_z] | jm \rangle_{m=j} \mu_N = j \left( g_l \pm \frac{g_s - g_l}{2l + 1} \right) \mu_N \quad (7)$$

for  $j = \ell \pm 1/2$ . If the free nucleons  $g$  factors are used, this single-particle moment is called the Schmidt moment. The single-particle intrinsic spin expectation value  $\langle s \rangle_{sp}$  is  $+\frac{1}{2}$  for  $j = \ell + 1/2$  and  $-\frac{1}{2} \frac{2\ell-1}{2\ell+1}$  for  $j = \ell - 1/2$ .

For the odd-odd  $^{32}\text{Cl}$  nucleus, the Schmidt moment resulting from the assumed single-particle configuration  $(\nu s_{1/2} \otimes \pi d_{3/2})_{1-}$  is given by

$$\mu_{sp}(J = 1) = -\left(\frac{1}{2}\right)\mu_{sp}(s_{1/2}) + \left(\frac{5}{6}\right)\mu_{sp}(d_{3/2}) \quad (8)$$



Using the single-particle moments for an  $s_{1/2}$  neutron  $\mu_{sp} = -1.913\mu_N$  and for a  $d_{3/2}$  proton  $\mu_{sp} = 0.124\mu_N$ , we find  $\mu_{sp}({}^{32}\text{Cl}) = 1.060\mu_N$ . When compared to the present experimental value of  $1.114(6)\mu_N$  one might conclude that the configuration of this state is close to the single-particle value. However, a more complete comparison (see Table I) with the magnetic moments for the neighboring nuclei  ${}^{31}\text{S}$  and  ${}^{33}\text{Cl}$  with  $T = 1/2$  which have the  $J^\pi$  values for  $s_{1/2}$  and  $d_{3/2}$ , respectively, shows that Schmidt values are actually far from the experimental situation. The same conclusion is obtained from the mirror nuclei  ${}^{31}\text{P}$ ,  ${}^{33}\text{S}$ , and  ${}^{32}\text{P}$ ; see Table I. If the experimental single-particle moments of  ${}^{31}\text{S}$  and  ${}^{33}\text{Cl}$  [16] are used in (7), we find  $\mu_{eff}({}^{32}\text{Cl}) = 0.871\mu_N$ , very different from the measured value.

A better understanding of the magnetic moments comes from the full  $(1s_{1/2}, 0d_{5/2}, 0d_{3/2})$  ( $sd$ )-shell model basis [17]. We have calculated wave functions and magnetic moments with several effective  $sd$ -shell Hamiltonians. The Hamiltonians consist only of one- and two-body parts, and are therefore defined by specification of all one-body (3) and two-body (63) matrix elements which can be formed with all of the active orbits in the  $sd$ -shell. Diagonalization of the Hamiltonian matrix then yields the set of mixed configuration shell-model wave functions which are used to calculate magnetic moments. For  ${}^{32}\text{Cl}$ ,  $1^+$  the matrix dimension is 1413.

We first compare with results based on the USD Hamiltonian of Wildenthal. The USD Hamiltonian was derived starting from a renormalized G matrix, and then the linear combinations of two-body matrix elements which can be determined from a large set (about 450) of binding energy and excitation energy data for the  $sd$ -shell nuclei ( $A = 16 - 40$ ) [17]. The magnetic moments for  $A = 31 - 33$  obtained with this Hamiltonian and the free-nucleon  $g$  factors are compared with experiment in Table I (USD-free). The agreement with experiment is greatly improved compared to the Schmidt values. The single-particle configuration assumed for the Schmidt value calculation is in fact only about 50% of the full  $sd$ -shell wave function. The remaining 50% of the full wave function is a complex mixing of many configurations. The deviations between the experimental and USD-free values is up to  $0.2\mu_N$ . The isoscalar magnetic moments calculated for the  $T = 0$  multiplets appear to be in better agreement with theory; however, this is due to the trivial  $J$  factor which

appears in Eq. (4). When Eq. (4) is used to deduce the scalar spin expectation value (the last three rows of Table I) the non-trivial part of the deviation is emphasized.

It has been suggested [18] that isospin mixing may be responsible for the anomalous scalar spin expectation value for the  $A = 9, T = 3/2$  mirror pair [18,19]. We have calculated the  $A = 31 - 33$  magnetic moments using the isospin nonconserving Hamiltonian of [20] and find changes of only about  $0.01 \mu_N$  in the magnetic moments. We conclude that isospin mixing is not important at the level of the remaining deviation between experiment and theory.

The  $M1$  and Gamow-Teller (GT) data throughout the  $sd$ -shell show clear evidence for renormalization of the  $M1$  and GT operator due to higher-order configuration mixing and mesonic exchange currents. Data for  $M1$  and GT observables in the  $sd$ -shell have been compared to the USD-free predictions in order to determine the best overall set of effective  $g$  factors [14,15,21]. These are close to but not in perfect agreement with microscopic calculations of the higher-order and mesonic exchange effects. For the GT decay, the renormalization shows up clearly as a reduction (quenching) of the experimental Gamow-Teller strength to about 60% of their calculated values [21]. The same reduction factor ( $\sqrt{0.6}$ ) must enter into the isovector spin part of the isovector moments. However, there is also a mesonic exchange enhancement in the isovector orbital operator [15]. The consequence of this is that the magnetic moments in the  $sd$ -shell are (accidentally) close to the free-nucleon results and that the effect of the renormalization on the  $M1$  operator is more complex.

The magnetic moment data for  $A = 31 - 33$  are compared with those calculated with the effective  $M1$  operator of Ref. [15] in Table I (USD-eff). In most cases there is some improvement over USD-free when compared to experiment. However, the changes are not large (due to the reason discussed above) and there is still about the same overall deviation between experiment and theory. The rather small difference between USD-free and USD-eff is due to the complexity of the actual  $sd$ -shell wave functions. As a contrasting situation where the wave function is simple, we can compare the experimental moment of 0.391 for  $^{39}\text{K}$  to its USD-free value of 0.124 (which is the same as the Schmidt value) and USD-eff

value of 0.381.

The complexity of the wave functions in the  $A = 31 - 33$  region means that the results are sensitive to the  $sd$ -shell Hamiltonian. There are two other “universal”  $sd$ -shell Hamiltonians we can examine; the SDPOTA and SDPOTB Hamiltonians from Ref. [22]. These are based upon adjusting the strengths of density-dependent one-boson exchange potentials. Both Hamiltonians have 17 potential parameters, and they differ by how the mass dependence of the single-particle energies are treated. The overall description of the binding energies and excitation energies for the entire  $sd$ -shell is about the same as for USD. Comparison of USD, SDPOTA and SDPOTB results gives an indication of the sensitivity of the magnetic moments to the small and energetically undetermined parts of the  $sd$ -shell Hamiltonian. The results for these three Hamiltonians and with the effective  $M1$  operator are compared to experiment in Table I. We see that there are variations of up to  $0.20\mu_N$  due to the Hamiltonian. Overall, experiment is in best agreement with SDPOTA, with remaining differences with experimental moments on the order of  $0.06\mu_N$ . This is typical of the deviation between the entire set of  $sd$ -shell moments with those obtained with the USD-eff [17,23]. We would conclude that the SDPOTA Hamiltonian is better for the  $A = 31 - 33$  mass region. However to make a general conclusion about the Hamiltonian, one needs to carry out a comparison between  $M1$  observables and those calculated with SDPOTA for other  $sd$ -shell nuclei. In general one can conclude that magnetic moment data are an important ingredient in testing and determining the effective Hamiltonian.

In summary, the magnetic moment of  $^{32}\text{Cl}$  has been successfully measured by means of conventional  $\beta$ -NMR spectroscopy, completing the mass 32 isospin  $T = 1$  system. A comparison of its value with magnetic moments of neighboring  $A = 31$  and 33 nuclei shows that the apparent agreement between Schmidt prediction and experiment is accidental. According to shell model calculations the single-particle configuration assumed for the Schmidt prediction is only about 50% of the full  $sd$ -shell wave function, the remaining 50% being a complex mix of many configurations. Of the shell-model calculations presented here, the SDPOTA Hamiltonian results are in best agreement with the data for this mass region.

#### IV. ACKNOWLEDGMENTS

This work was supported in part by the National Science Foundation grant PHY95-28844. The authors would like to thank the NSCL operations staff for providing the primary and secondary beams for this experiment. WFR was supported by NSF grant PHY97-22692, BAB was supported by NSF grant PHY96-05207, and GN is a post-doctoral researcher of the FWO-Vlaanderen.

## REFERENCES

- [1] L. Pfeiffer and L. Madansky, *Phys. Rev.* **163**, 999 (1967).
- [2] Y. Yamazaki, O. Hashimoto, H. Ikezoe, S. Nagamiya, K. Nakai, and T. Yamazaki, *Phys. Rev. Lett.* **33**, 1614 (1974).
- [3] W.F. Rogers, D.L. Clark, S.B. Dutta, and A.G. Martin, *Phys. Lett.* **B177**, 293 (1986).
- [4] K. Asahi, M. Ishihara, N. Inabe, T. Ichihara, T. Kubo, M. Adachi, H. Takanashi, M. Kouguchi, M. Fukuda, D. Mikolas, D.J. Morrissey, D. Beaumel, T. Shimoda, H. Miyatake, and N. Takahashi, *Phys. Lett.* **B251**, 488 (1990).
- [5] K. Matsuta, A. Ozawa, Y. Nojiri, T. Minamisono, M. Fukuda, A. Kitagawa, S. Momota, T. Ohtsubo, Y. Matsuo, H. Takechi, S. Fukuda, I. Minami, K. Sugimoto, I. Tanihata, K. Omata, J.R. Alonso, G.F. Krebs, and T.J.M. Symons, *Phys. Lett.* **B281**, 214 (1992)
- [6] E. Arnold, J. Bonn, A. Klein, R. Neugart, M. Neuroth, E.W. Otten, P. Lievens, H. Reich, W. Widdra, and the ISOLDE Collaboration *Phys. Lett.* **B281**, 16 (1992).
- [7] M. Lindroos and the ISOLDE Collaboration, *Nucl. Instrum. Meth. in Phys. Res. B* **126**, 423 (1997).
- [8] E. Arnold, J. Bonn, W. Neu, R. Neugart, E.W. Otten, and the ISOLDE Collaboration, *Z. Phys.* **A331**, 295 (1998).
- [9] P.F. Mantica, R.W. Ibbotson, D.W. Anthony, M. Fauerbach, D.J. Morrissey, C.F. Powell, J. Rikovska, M. Steiner, N.J. Stone, and W.B. Walters, *Phys. Rev.* **C55**, 2501 (1997).
- [10] C. Detraz, C.S. Zaidins, D.J. Frantsvog, R.L. Wilson, and A.R. Kunselman, *Nucl. Phys.* **A203**, 414 (1973).
- [11] Formulae for this calculation can be found in “Low-Temperature Nuclear Orientation”, eds. H. Postma and N.J. Stone (North Holland, Amsterdam, 1986). Chapter 3.

- [12] B. Castel and I.S. Towner, "Modern theories of nuclear moments" (Clarendon Press, Oxford, 1990).
- [13] K. Sugimoto, Phys. Rev. **182**, 1051 (1969).
- [14] B.A. Brown and B.H. Wildenthal, Phys. Rev. **C28**, 2397 (1983).
- [15] B.A. Brown and B.H. Wildenthal, Nucl. Phys. **A474**, 290 (1987).
- [16] P. Raghavan, At. Data and Nucl. Data Tables **42**, 189 (1989).
- [17] B.A. Brown and B.H. Wildenthal, Ann. Rev. Nucl. Part. Sci. **38**, 29 (1988).
- [18] M. Huhta, P.F. Mantica, D.W. Anthony, B.A. Brown, B.S. Davids, R.W. Ibbotson, D.J. Morrissey, C.F. Powell, and M. Steiner, Phys. Rev. **C57**, R2790 (1998).
- [19] K. Matsuta, T. Minamisono, M. Tanigaki, M. Fukuda, Y. Nojiri, M. Mihara, T. Onishi, T. Yamaguchi, A. Harada, M. Sasaki, T. Miyake, K. Minamisono, T. Fukao, K. Sato, Y. Matsumoto, T. Ohtsubo, S. Fukuda, S. Momota, K. Yoshida, A. Ozawa, T. Kobayashi, I. Tanihata, J.R. Alonso, G.F. Krebs and T.J.M. Symons, Hyp. Int. **97/98**, 519 (1996).
- [20] W.E. Ormand and B.A. Brown, Nucl. Phys. **A491**, 1 (1989).
- [21] B.A. Brown and B.H. Wildenthal, At. Data Nucl. Data Tables **33**, 347 (1985).
- [22] B.A. Brown, W.A. Richter, R.E. Julies, and B.H. Wildenthal, Ann. Phys. **182**, 191 (1988).
- [23] A. Klein, B.A. Brown, U. Georg, M. Keim, P. Lievens, R. Neugart, M. Neuroth, R.E. Silverans, L. Vermeeren, and the ISOLDE Collaboration. Nucl. Phys. **A607**, 1 (1996).

## FIGURES

FIG. 1. Schematic of the NSCL  $\beta$ -NMR apparatus.

FIG. 2. Resonance curves obtained for  $^{32}\text{Cl}$  implanted in NaCl. The applied frequency modulation was (a)  $\pm 25$  kHz, and (b)  $\pm 10$  kHz. The RF modulation had a ramp waveform with a 500 Hz repetition rate.

TABLES

TABLE I. Experimental and calculated magnetic moments for the  $A = 31 - 33$  isospin multiplets. The calculated moments are based on the Schmidt value and on the full  $sd$ -shell basis with three effective Hamiltonians USD, SDPOTA and SDPOTB. The  $M1$  operator is evaluated with the free-nucleon and the effective  $sd$ -shell operator of Ref. [15]. Experimental data are from [16] and this work.

Hamiltonian			exp	Schmidt	USD	USD	SDPOTA	SDPOTB	
$M1$ operator					free	eff	eff	eff	
Nucleus	$T_z$	$I^\pi$							
$\mu$	$^{31}\text{S}$	+1/2	$1/2^+$	-0.488	-1.913	-0.400	-0.431	-0.547	-0.591
	$^{33}\text{Cl}$	+1/2	$3/2^+$	0.752	0.124	0.704	0.799	0.730	0.796
	$^{32}\text{Cl}$	+1	$1^+$	1.114(6)	1.060	1.006	1.157	1.177	1.232
$\mu$	$^{31}\text{P}$	-1/2	$1/2^+$	1.235	2.793	1.023	1.086	1.241	1.288
	$^{33}\text{S}$	-1/2	$3/2^+$	0.644	1.148	0.651	0.643	0.724	0.659
	$^{32}\text{P}$	-1	$1^+$	-0.252	-0.440	-0.131	-0.238	-0.308	-0.348
$\mu^v$	$A = 31 (T = 1/2)$		$1/2^+$	-0.862	-2.353	-0.711	-0.758	-0.894	-0.939
	$A = 33 (T = 1/2)$		$3/2^+$	0.054	-0.512	0.026	0.078	0.003	0.069
	$A = 32 (T = 1)$		$1^+$	0.683	0.750	0.568	0.697	0.742	0.790
$\mu^s$	$A = 31 (T = 1/2)$		$1/2^+$	0.373	0.440	0.311	0.328	0.347	0.348
	$A = 33 (T = 1/2)$		$3/2^+$	0.698	0.636	0.678	0.721	0.727	0.727
	$A = 32 (T = 1)$		$1^+$	0.431	0.310	0.438	0.460	0.434	0.442
$\langle s \rangle$	$A = 31 (T = 1/2)$		$1/2^+$	0.324	0.500	0.162	0.204	0.255	0.259
	$A = 33 (T = 1/2)$		$3/2^+$	-0.137	-0.300	-0.191	-0.076	-0.060	-0.060
	$A = 32 (T = 1)$		$1^+$	-0.182	-0.500	-0.164	-0.107	-0.172	-0.153



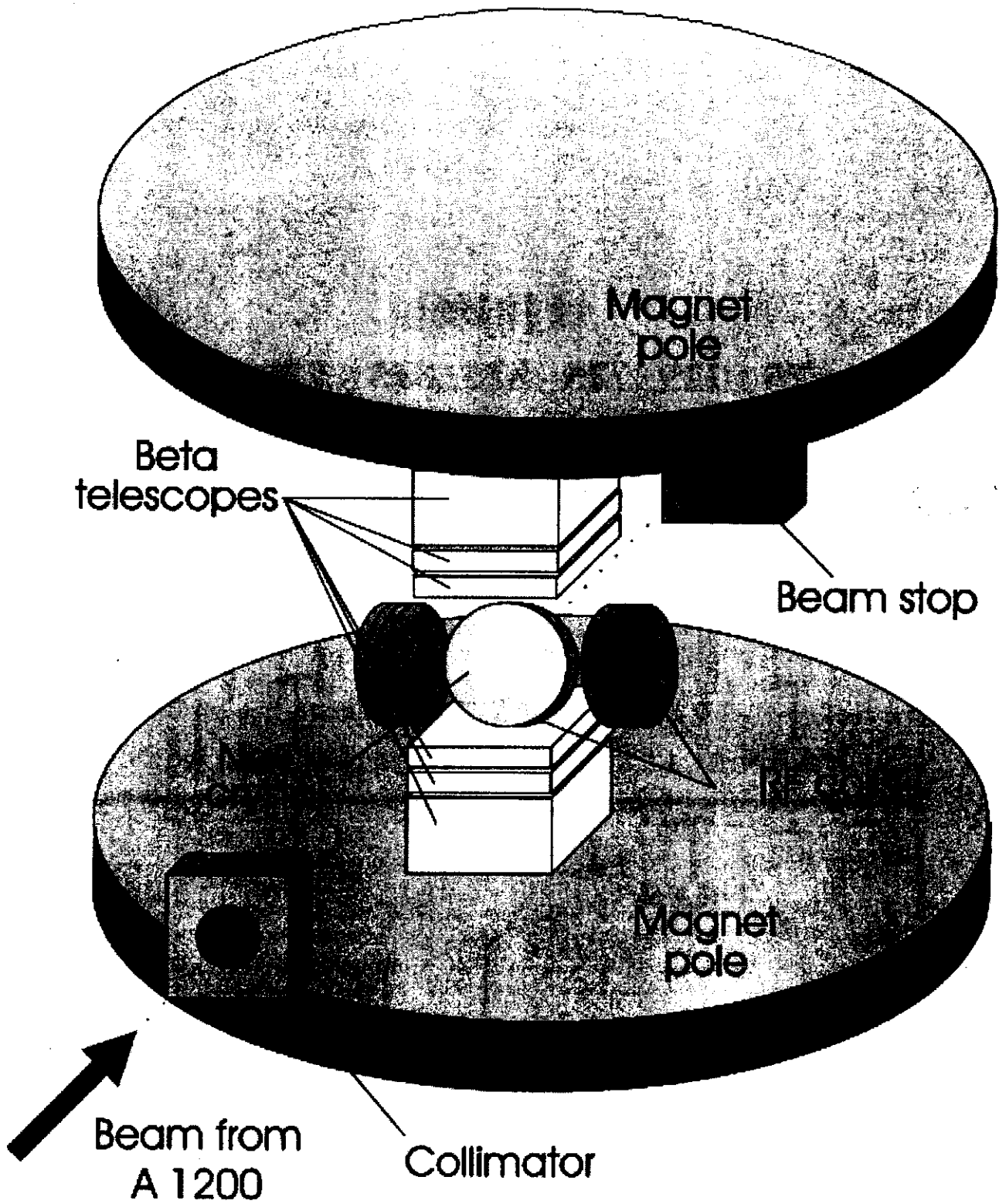


Fig 1

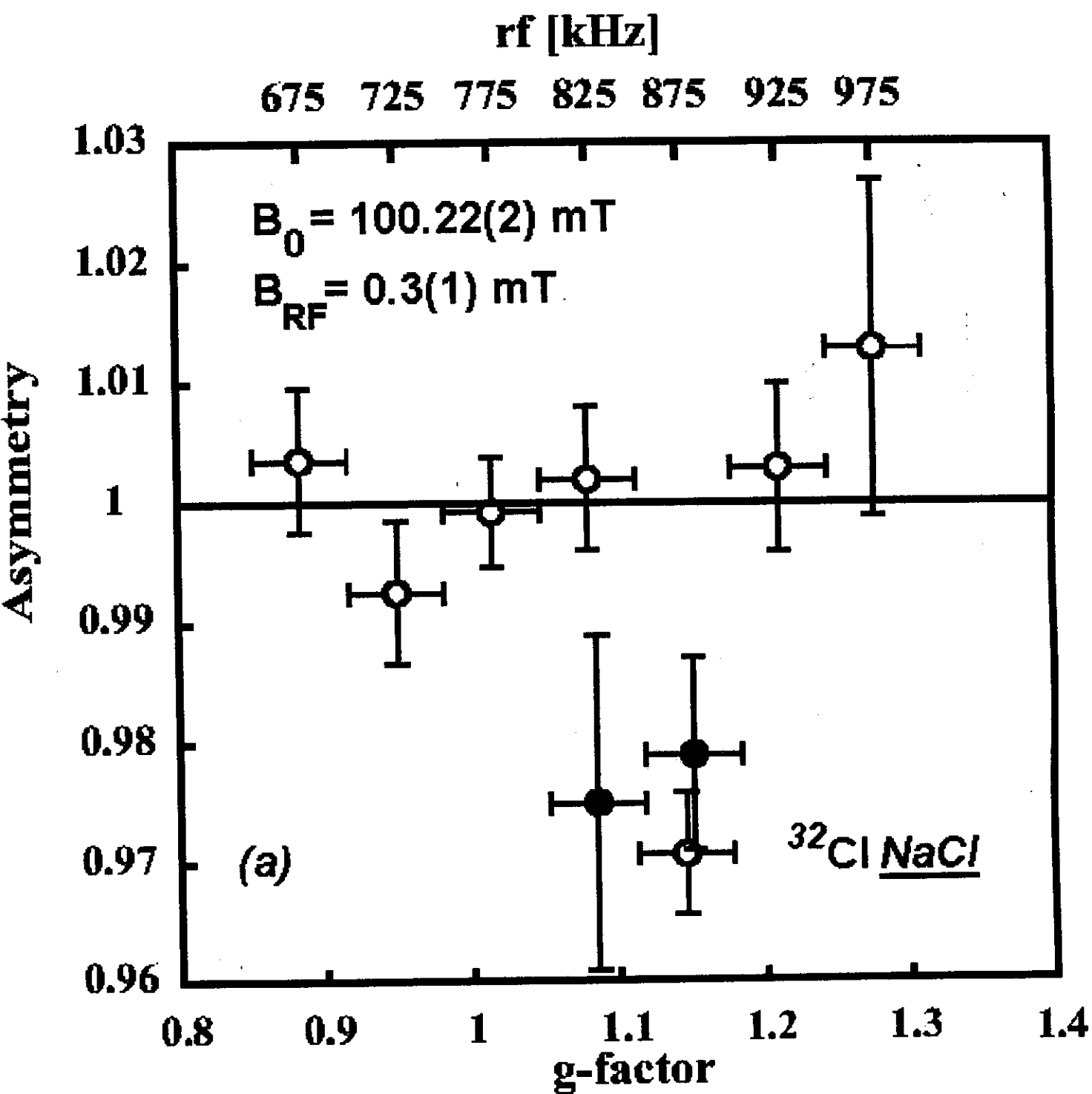


Fig 2a

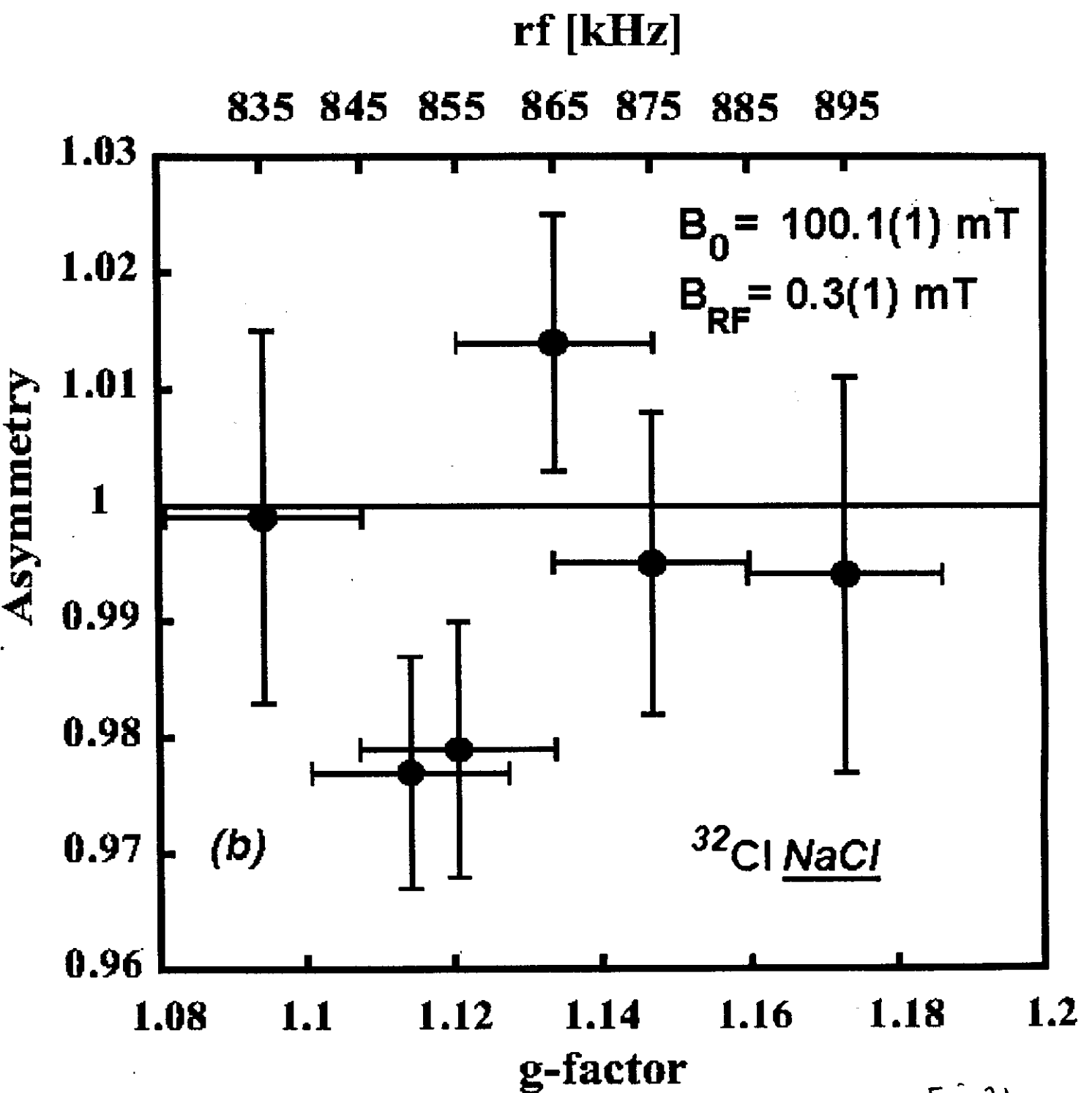


Fig 2b